Available online at www.sciencedirect.com
ScienceDirect
Journal of Photochemistry and Photobiology A: Chemistry 191 (2007) 104–113
Journal of Photochemistry and Photobiology A:Chemistry
www.elsevier.com/locate/jphotochem

Study on interaction between apigenin and human serum albumin by spectroscopy and molecular modeling

Jiang-Lan Yuan [a,b], Zhong lv [a], Zhi-Gang Liu [b], Zheng Hu [b], Guo-Lin Zou [a,*]

[a] *Key Laboratory of MOE for Virology, College of Life Sciences, Wuhan University, Wuhan 430072, PR China*
[b] *Biological Engineering College, HuBei University of Technology, Wuhan 430064, PR China*

Received 18 January 2007; received in revised form 18 March 2007; accepted 9 April 2007
Available online 13 April 2007

Abstract

Apigenin (Ap) is one of the most common dietary flavonoids, and possesses extensive bioactivities. In our work, interaction of Ap and human serum albumin (HSA) had been investigated systematically by fluorescence spectroscopic, circular dichroism (CD), UV–vis absorption spectroscopic and molecular modeling. The results indicated that binding of Ap to HSA caused strong fluorescence quenching of HSA through static quenching mechanism, hydrophobic and electrostatic interaction are the predominant forces in the Ap–HSA complex, and the process of Ap binding HSA was droved by enthalpy ($\Delta H = -17.497\,\mathrm{kJ\,mol^{-1}}$) and entropy ($\Delta S = 37.04\,\mathrm{J\,mol^{-1}}$). The results from synchronous fluorescence showed that microenvironment around tyrosine (Tyr) had a slight trend (about blueshift of 1 nm) of polarity decreasing. The formation of the complex had not changed the secondary structure of HSA by CD. The binding distance r between donor (HSA) and acceptor (Ap) is 3.21 nm according to the theory of Förster resonance energy transfer. By method of molecular modeling, Ap was located to the entrance of site I by hydrophobic and electrostatic forces, which matched exactly the corresponding experimental results.

Keywords: Apigenin; Human serum albumin; Interaction; Spectroscopy; Modeling

1. Introduction

Flavonoid exists widely in vegetable kingdom as polyphenolic compounds. Some evidences show that a flavonoid-rich diet inversely correlates with the risk of coronary heart disease or carcinogenesis [1]. In recently decades, investigation on flavonoid is mainly focused on their physiological and pharmacological function and many publications suggest that flavonoid possess multiple beneficial biological effects

Ap named as 4′,5,7-trihydroxyflavone (Fig. 1) is one of the most common dietary flavonoids, non-toxic and non-mutagenic, and is widely distributed in many fruits and vegetables including parsley, onions, orange, tea, wheat sprouts and so on [2]. As an important food functional factor and potential therapeutic drug for some diseases it has been widely investigated. Many literatures showed that Ap possesses the extensive bioactivities such as anti-inflammatory [3], cardiovascular effects [4], scavenging free radical, lowering blood pressure [4], antitumor [5], antispasmodic [6], antidiarrhoeal [7], antiproliferative activities[8–10], inducing apoptosis[11–14], chemoprevention and cancer chemotherapy [15–17]. However, little work has been carried out on the absorption, metabolism, and transportation of Ap up to date.

Human serum albumin (HSA) as a kind of main carrier protein is the most abundant in human blood plasma (approximately 5 g/100 mL)and provide about 80% of the osmotic pressure of blood [18]. HSA has a high affinity to an extraordinarily diverse range of materials such as drugs, metabolites, fatty acids and metal ions, so it serves as a solubilizer and transporter for the materials. As a kind of storage form of chemicals, it plays an important role on transportation of drug and other exogenous and endogenous compounds to their targets. HSA have been used as a model protein for many and diverse biophysical and physicochemical studies.

This study on the interaction of drugs to HSA is helpful for realizing the distribution and transportation of drugs in vivo,

Abbreviations: HSA, human serum albumin; Ap, apigenin; UV–vis, ultraviolet visible absorbance spectroscopy; CD, circular dichroism

* Corresponding author. Tel.: +86 27 87645674; fax: +86 27 68752560.
E-mail address: zouguolin@whu.edu.cn (G.-L. Zou).

1010-6030/$ – see front matter © 2007 Published by Elsevier B.V.
doi:10.1016/j.jphotochem.2007.04.010

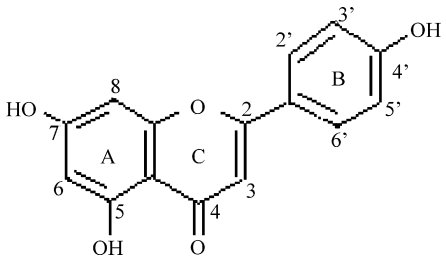

Fig. 1. Chemical structure of Ap.

elucidating action mechanism, toxicity and dynamics of drugs at the molecular level. So far, no investigation in detail about Ap binding HSA is carried out. In this work, mechanisms and characters of interaction between Ap and HSA were investigated systematically by spectroscopic and molecular modeling methods.

2. Materials and methods

2.1. Materials

Ap and HSA (66,000 Da) was obtained from Sigma Chemical Company (USA), Tris base was from Amersco (Japan), all agents were all of analytical purity. The buffer solution was consisted of 20 mmol L^{-1} Tris–HCl and 0.15 mol L^{-1} NaCl, pH of which was 7.4. The 2.0×10^{-5} mol L^{-1} stock solution of HSA was always prepared freshly in the buffer, 0.01 mol L^{-1}. Ap was stocked in ethanol and was diluted to the experimental concentration with the buffer. Ultra purity water was used throughout.

2.2. Apparatus and methods

Fluorescence spectra and data was recorded from 290 to 500 nm on F-4500 Fluorescence Spectrophotometer (Hitachi, Tokyo, Japan) with a 1.0 cm quartz cell and thermostat bath, the widths of excitation and emission slit were set at 5.0 nm. The UV–vis absorption measurements were performed on a double beam Cary 100 UV–vis Spectrometer (Varian, USA) with a 1.0 cm quartz cell at room temperature.

The CD spectra were gained by JASCO J-820 Automatic Recording Spectropolarimeter (Japan Spectroscopic Company, Japan) with a 0.1 cm quartz cell at room temperature, the speed of scanning was 20 nm min^{-1}, the slit width was set at 5 nm. The samples were prepared beforehand, then added into a 0.1 cm quartz cell to be determined. The concentration of HSA was 5.0 μM, the buffer as common baseline of all samples was subtracted during scanning. Each sample was scanned for three times to average for a CD spectrum.

2.3. Procedures of fluorescence measurement

A 2.0 mL of 1.0 μmol L^{-1} HSA solution was added accurately into an 1.0 cm quartz cell, and then was titrated by successive additions of 1.0×10^{-3} mol L^{-1} Ap with 2 μL trace syringe to attain a series of final concentrations. Titrations were operated manually and mixed moderately. When experiments about temperature (288, 298 and 308 K) were carried out, pH was justified to 7.4 by 0.1 mol L^{-1} NaOH or HCl at every temperature stabilized by recycle water from thermostat bath. The spectra about pH experiment were scanned at two pH (8.4, 7.2) and $T = 293$ K. Every case of all experiments was in the same buffer mentioned above.

2.4. Analysis of HSA fluorescence quenching

Most proteins can emit intrinsic fluorescence after absorbing ultraviolet as a result that there are some residues such as Trp, Tyr and Phe in their molecular structure, so is HSA. The fluorescence intensity of protein can be weakened by a variety of molecular interaction, which is called fluorescence quenching. Degree of fluorescence quenching suggests the change of protein structure and microenvironment around the residues above. The Stern–Volmer equation is often applied to describe the fluorescence quenching:

$$\frac{F_0}{F} = 1 + K_q\tau_0[Q] = 1 + K_{SV}[Q] \quad (1)$$

In the Eq. (1), F_0 and F are the fluorescence intensity before and after quencher adding, respectively, K_{SV} is the Stern–Volmer dynamic quenching constant, a direct measure of the quenching efficiency, and K_q is the quenching rate constant of biomolecule, τ_0 and $[Q]$ are the average lifetime of biomolecule and concentration of quencher, respectively [19]. Obviously, the value of K_q is educed by the equation as follow:

$$K_{SV} = K_q\tau_0 \quad (2)$$

where the τ_0 is 10^{-8} s and K_{SV} is the slope of linear regressions of curve of F_0/F versus $[Q]$. By K_q and K_{SV}, mechanism of fluorescence quenching can be learned.

The apparent constant K_A and binding sites n can be elicited from the following equation:

$$\log(F_0 - F)/F = n \log K_A - n \log(1/[D_t] - (F_0 - F)[P_t]/F_0)) \quad (3)$$

In Eq. (3), n is the number of binding sites, and $[D_t]$ and $[P_t]$ are the total concentration of quencher and protein, respectively, n can be educed from the slope of linear regressions of the curve $\log(F_0 - F)/F$ versus $\log(1/([D_t] - (F_0 - F)[P_t]/F_0))$ and K_A is deduced from the intercept of the linear regressions.

The values of enthalpy change (ΔH) and entropy change (ΔS) can be measured from the Van't Hoff equation:

$$\ln K_A = -\frac{\Delta H}{RT} + \frac{\Delta S}{R} \quad (4)$$

And the free energy change (ΔG) can be estimated from the following typical thermodynamics equation:

$$\Delta G = \Delta H - T\Delta S \quad (5)$$

2.5. Principles and calculations of molecular modeling [20–22]

Molecular modeling is obtained by technique of molecule docking computing in which ligands are located to the active site of the corresponding receptor and then to evaluate the interaction and educe the most possible modeling according to the principles of the lowest energy combined with matching quality geometrically between ligand and receptor.

The program AutoDock 3.05 was applied to study molecule docking, in which an improved heredity computing method, Lamarckian genetic algorithm (LGA), is used to find the optimum binding site and evaluate the matching degree between ligand and receptor by the calculating method of semi-empirical free energy.

The 3D structure of Ap was calculated and optimized by applying the tripos force field with gasteiger-Hückel charges from software Sybyl 6.9.2. The crystal structure of HSA entitled 1H9Z was taken from the Brookhaven Protein Data Bank (http://www.rcsb.org/pdb) [19]. The structure of HSA was assigned according to the Amber 4.0 force field with Kollman-united-atom charges encoded in Sybyl 6.9.2[20]. The solution parameters were added to protein using Addsol modules of AutoDock. The MOLCAD implemented in Sybyl 6.9.2 software package was used to visualize the environment of binding pocket. Molecular modeling was carried out on a 16 CPU SGI workstation.

3. Results and discussions

3.1. UV spectral properties of Ap

The UV–vis spectra of Ap at different pH (6.4,7.4,8.4) in the buffer were illustrated in Fig. 2. In the spectral range of 225–500 nm Ap show two main absorption bands (band I, 310–350 nm; band II, 260–310 nm). It is very obvious that decreasing of pH caused the dramatic weakening of band I and sudden enhancing of band II. The possible reason is that the phenolic hydroxyl groups of Ap in the 5, 7, 4′ positions can be dissociated incompletely and the equilibrium about dissociating is effected by value of pH, so formed the mixture of neutral and anionic species. Ap, as a kind of polyphenolic compound, can dissociate theoretically and arrive at a dynamic equilibrium at certain conditions. According to the dissociation of other phenolic compound, the possible mechanism of dissociation is:

$$\mathrm{Ap} + \mathrm{H_2O} = [\mathrm{Ap}]^- + \mathrm{H_3O^+} \quad \text{(a)}$$

$$[\mathrm{Ap}]^- + \mathrm{H_2O} = [\mathrm{Ap}]^{2-} + \mathrm{H_3O^+} \quad \text{(b)}$$

$$[\mathrm{Ap}]^{2-} + \mathrm{H_2O} = [\mathrm{Ap}]^{3-} + \mathrm{H_3O^+} \quad \text{(c)}$$

As can be seen from Eqs. (a), (b) and (c), the increasing of pH is helpful apparently for the dissociation of Ap. Regularly, the dissociation from the first step, that is to say, Eq. (a) is predominant, so $[\mathrm{Ap}]^-$ should be the most main anionic species in the solution. The UV absorption characters of Ap at different pH suggested that band I is resulted from anionic species and band II from neutral molecule of Ap. Generally, neutral and anionic species coexist in dynamic equilibrium.

As showed in Fig. 3, the absorption intensity of Ap at 202 nm lowered regularly and the position of peaks shifted from 202 to 224 nm along with increasing of HSA but no obvious change for the peak at 323 nm, which give an original evidence that there was interaction between Ap and HSA. C. D. Kanakis reported that characteristic UV absorption bands of quercetin at 374 nm, kaempferol at 368 nm and delphinidin at 572 nm were observed obvious reduction of intensity and redshift after binding to HSA, which indicated the change of a major pigment structure in these flavonoid–HSA complexes [23]. The decrease in absorption intensity suggests that quercetin binds HSA in ionic form in non-planar conformation [23,24]. HSA had no effect on the pigment structure of Ap but alter the microenvironment around Ap and hint Ap contact molecular of HSA.

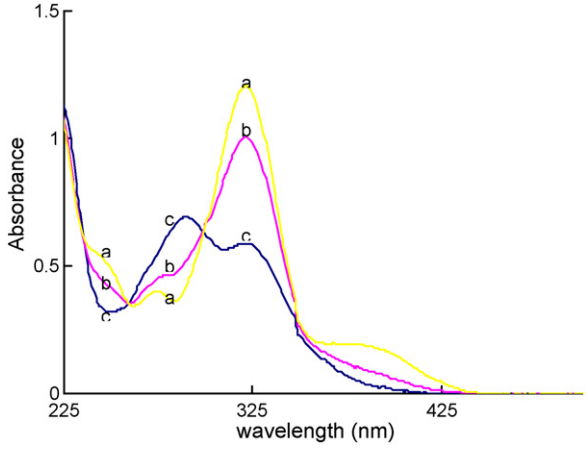

Fig. 2. UV–vis absorption spectra of Ap at different pH: (a) 8.4; (b) 7.4; (c) 6.4 in the 20 mmol L^{-1} Tris–HCl buffer, [Ap] = 50 μmol L^{-1}, T = 288 K.

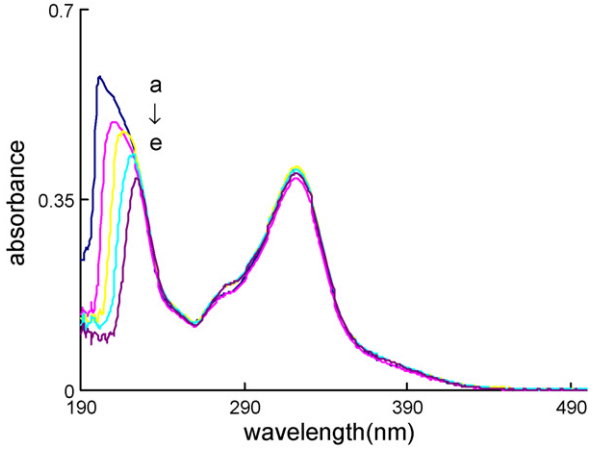

Fig. 3. UV–vis absorption spectra of Ap without and with HSA. Subtracting the corresponding spectrum of HSA in the buffer, respectively. Concentration of HSA was 0, 1, 2, 3, 4 μmol L^{-1} from the (a)–(e) with 20 μmol L^{-1} Ap in the 20 mmol L^{-1} Tris–HCl buffer, pH 7.4, T = 288 K.

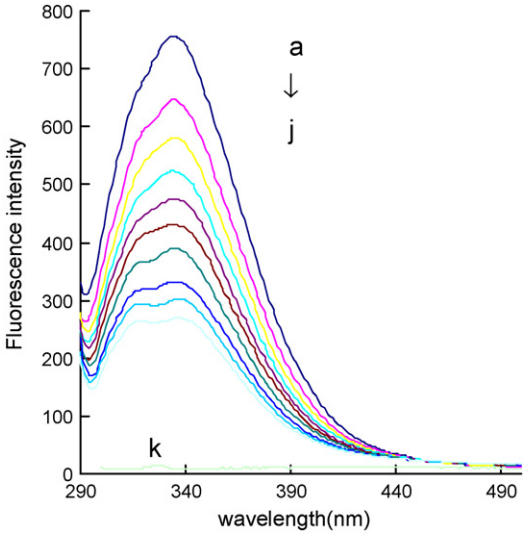

Fig. 4. Fluorescence spectra of Ap–HSA system. Concentration of HSA was 1.0 μmol L^{-1} while the corresponding concentrations of Ap were 0, 0.5, 1.0, 2.0, 3.0, 4.0, 6.0, 8.0, 10.0, 12.0 μmol L^{-1} from the (a)–(j), the curve k is the spectrum of 10 μmol L^{-1} Ap. T = 288 K, pH 7.4, λ_{ex} = 285 nm.

3.2. Fluorescence quenching of HSA induced by Ap

HSA is a single-string globular protein with 585 amide acids, in which 35 cysteines constitute 17 disulfide bridges and only in the 34th site of N terminal there is a –SH. 18 Tyr residues and 1 Trp residue in HSA are responsible for intrinsic fluorescence under excitation of ultraviolet.

HSA can emit strong intrinsic fluorescence at 334 nm when it was excited at 285 nm, and the sole Trp residue located at 214th of the chain and Tyr residues in HSA could explain the phenomenon. The characteristic that intrinsic fluorescence of HSA is very sensitive to its microenvironment was deserved to be regarded, when local surroundings of HSA was altered slightly its intrinsic fluorescence would weaken obviously, such factors as protein conformational transition, biomolecule binding, and denaturation, etc. are responsible for the weakening.

The fluorescence quenching of HSA induced by Ap is showed in Fig. 4. Obviously, the fluorescence intensity of HSA weakened regularly with the increasing of Ap concentration. In the experiment, the pH value was stabilized at 7.4 and the temperature was below 308 K, so it is impossible to denature HSA. The possible factors of fluorescence quenching were the alteration of HSA conformation and/or the binding of Ap to HSA to result in fluorescence energy transferring from Tyr and/or Trp of HSA to Ap. The quenching indicates that Ap bind to HSA and the binding site is situated near the Trp^{214} and/or Tyr, so cause the decrease of fluorescence quantum yield in HSA.

3.3. Quenching mechanism

To investigate the quenching mechanism, the experiment about temperature and pH was carried out. Degree of fluorescence quenching of HSA weakened with temperature increasing and pH reducing. The Stern–Volmer linear curves for the binding of Ap to HSA are displayed in the Fig. 5. At every experimental

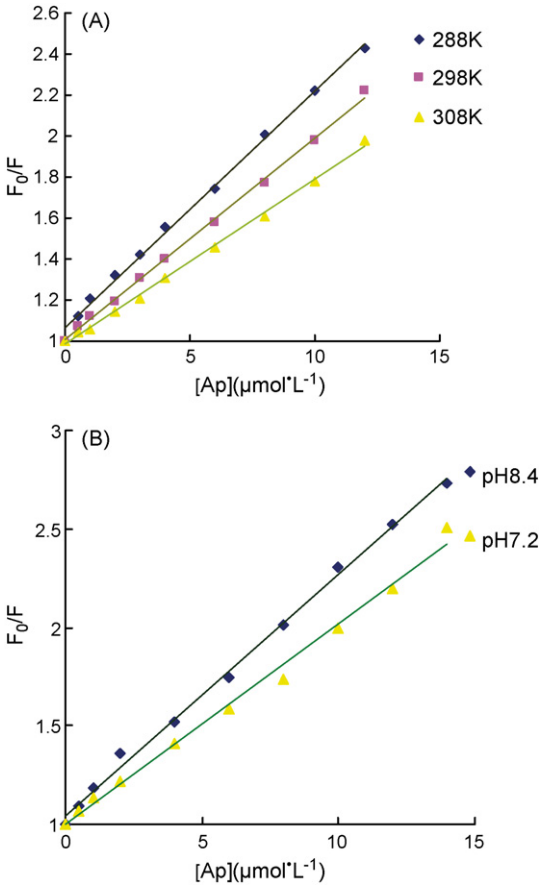

Fig. 5. The Stern–Volmer curves for the binding of Ap to HSA (A) at 288 K (♦), 298 K (■), 308 K (▲). (B) at pH 8.4 (♦) and 7.2 (▲) when T = 293 K. [HSA] = 1.0 μmol L^{-1}, λ_{ex} = 285 nm.

temperature and pH, the plots of F_0/F versus the concentration of Ap shows well linear relation, which indicates that the fluorescence quenching of HSA induced by Ap is either dynamic one or static one, i.e., only one kind of quenching mechanism is predominant [25].

The corresponding constants from Fig. 5 (A) and Eq. (1) are listed in Table 1. To compare with other biomolecules, the values of K_{sv} and K_q of Ap–HSA system are relatively high, suggesting high quenching efficiency. According to the Ref. [26], Ap contains the groups C (4′)–OH, C (4)=O and C (5)–OH, so it can interact strongly with HSA, and forming the Ap–HSA complex. The interaction between Ap and HSA resulted in the high quenching efficiency. The inverse correlation between Ksv and temperature indicated that the mechanism of the fluorescence quenching of HSA induced by Ap is not the dynamic but the static [27,28]. On the other hand, the maximum scatter collision quenching constant K_q for various quenchers with biomolecule

Table 1
Stern–Volmer quenching constants of Ap–HSA system at different temperatures

pH	T (K)	K_{sv} (10^4 L mol^{-1})	K_q (10^{12} L mol^{-1} s^{-1})	R
7.4	288	11.55	11.55	0.9981
	298	9.85	9.85	0.9991
	308	8.06	8.06	0.9989

Table 2
Stern–Volmer quenching constants of Ap–HSA system at different pH

T	pH	K_{sv} (10^4 L mol^{-1})	K_q (10^{12} L mol^{-1} s^{-1})	R	K_D (10^{-6} mol L^{-1})	R
293 K	8.4	12.22	12.22	0.9984	4.59	0.9975
	7.2	10.08	10.08	0.9966	4.16	0.9988

is 2.0×10^{10} L mol^{-1} S^{-1} [20,29]. In the study, K_q of binding of Ap with HSA is much greater than the maximum value of collision quenching K_q and so it suggests that the quenching is caused mainly by the static, i.e. the formation of HAS–Ap complex, but not dynamic one. On account of free pervasion of Ap molecular, we can speculate that dynamic mechanism has a minor effect on the fluorescence quenching of HSA

3.4. Analyses of thermodynamic parameters and binding forces

Usually, there are four types of noncovalent forces to affect the interaction between biomolecule and HSA, including hydrophobic, hydrogen, van der Waals and electrostatic forces. To analyze the type of binding force between Ap and HSA, the corresponding binding constants and thermodynamic parameters were computed according to the experiments about temperature and pH. For static quenching, the dissociation binding constant K_D can be calculated by Eq. (6) [20,30]:

$$1/(F_0 - F) = 1/F_0 + K_D/F_0[Q] \quad (6)$$

The corresponding figure and data about pH are displayed in Fig. 6 and Table 2, respectively. HSA with positive charges on its surface can form strong complexes with negatively charged flavonoid. Increasing of K_{sv}, K_q and K_D with pH increasing give an indication that the degree of Ap ionization is increasing gradually with pH increasing in the solution with HSA and Ap and so promote the binding of Ap to HSA, and the conclusion could be drawn that electrostatic and/or hydrogen bond force is predominant for the interaction between Ap and HSA. The results from Section 3.1 provide the explanation that the more ionization of Ap at high pH value is helpful for the binding by static force.

Thermodynamic parameters ΔH, ΔS and ΔG (Table 3) are calculated according to Van't Hoff equation. The data indicate that the binding action between Ap and HSA is spontaneous, enthalpy and entropy are favorable for the reaction. From viewpoint of water structure, a positive ΔS value is a typical evidence for hydrophobic interaction. Moreover, electrostatic interactions between ions in aqueous solution are characterized by a positive ΔS value and a negative ΔH value [26,31,32]. According to the results of UV absorption characteristic of Ap at different pH, ionic and neutral species of Ap at physiological condition can coexist at the state of dynamic equilibrium, so it is possible that ionic species of Ap bind HSA by electrostatic force. The lower positive ΔS proved that hydrophobic force gave significant contribution to the interaction [27]. Whether is hydrogen bonding force involved in the interaction? The results of this work could not answer this question yet.

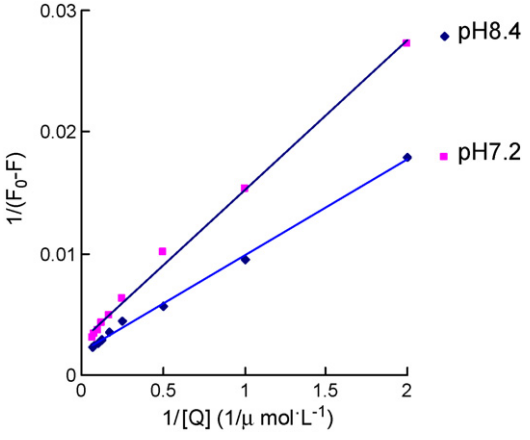

Fig. 6. The plots of $1/(F_0 - F)$ vs. $1/[Q]$ at pH 8.4 (♦), pH7.2 (▲). [HSA] = 1.0 μmol L^{-1}, λ_{ex} = 285 nm, λ_{em} = 334 nm, T = 293 K.

3.5. Binding parameters

Under the experimental temperatures and conditions, the conformation of HSA is not to be changed [27], and so the quenching by denaturizing can leave out of account. The plots of $\log(F_0 - F)/F$ versus $\log(1/([D_t] - (F_0 - F)[P_t]/F_0))$ at different temperatures and thermodynamic parameters of binding of Ap to HSA by them are presented in Fig. 7 and Table 3, respectively. It can be seen easily that K_A decreased but n increased along with the rising of temperature, illuminating that the interaction of Ap–HSA system belongs to radiative reaction and so the rising of temperature is not helpful for their binding. As a result of increasing of temperature, pervasion rate of Ap molecular quickens and the disorder of pervasion increases, consequently number of the binding site n increase. The conclusion was consistent with the results from thermodynamic analyses.

Table 3
The binding parameters and thermodynamic parameters of binding of Ap to HSA

pH	T (K)	n	$K_A \times 10^5$	R	ΔH (kJ mol^{-1})	ΔS (J mol^{-1})	ΔG (kJ mol^{-1})
7.4	288	0.728	1.297	0.9968	−17.497	37.04	−28.165
	298	0.8774	0.983	0.9967			−28.535
	308	1.0294	0.816	0.9969			−28.905

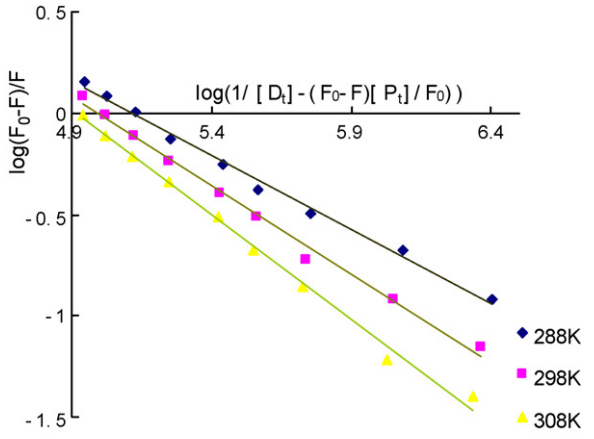

Fig. 7. The plots of log $(F_0 - F)/F$ vs. log$(1/([D_t] - (F_0 - F)[P_t]/F_0))$ at 288 K (♦), 298 K (■), 308 K (▲). [HSA] = 1.0 μmol L^{-1}, pH = 7.4, λ_{ex} = 285 nm, λ_{em} = 334 nm.

3.6. Energy transfer from HSA to Ap

A spectral overlap between the fluorescence spectra of free HSA and the UV–vis absorption spectra of Ap is displayed in Fig. 8. According to the Förster non-radiation energy transfer theory, the following typical equations can be used to analyze the problem about energy transfer [26,27,33]:

$$E = 1 - \frac{F}{F_0} = \frac{R_0^6}{(R_0^6 + r_0^6)} \quad (7)$$

$$R_0^6 = 8.79 \times 10^{-25} K^2 N^{-4} \emptyset J \quad (8)$$

$$J = \frac{\sum F(\lambda)\varepsilon(\lambda)\lambda^4 \Delta\lambda}{\sum F(\lambda)\Delta\lambda} \quad (9)$$

In the Eq. (7), E and r_0 mean the energy transfer efficiency and the distance between acceptor and donor, R_0 is the critical energy transfer distance at which 50% of the excitation energy is transferred to the acceptor, F and F_0 is the fluorescence intensity of donor without and with acceptor of the same concentration, respectively. K^2, N, $\emptyset$ and J in the Eq. (8) represent the spatial orientation factor describing the spatial orientation of the transition dipoles from donor to acceptor, the average refractive index for medium, the fluorescence quantum yield of the free donor and the overlap integral. $F(\lambda)$ and $\varepsilon(\lambda)$ is the fluorescence intensity of donor and the molar absorption coefficient of the acceptor at corresponding wavelength λ, respectively.

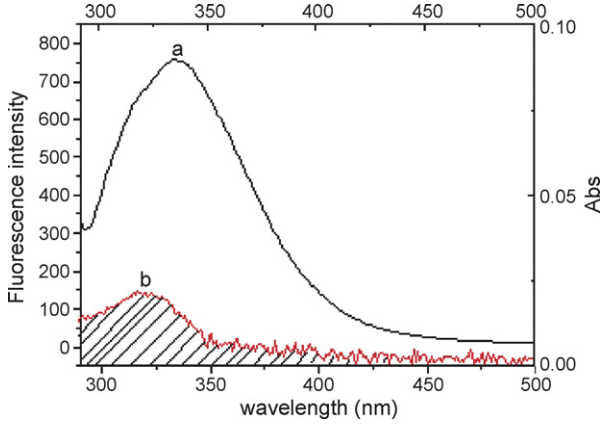

Fig. 8. Overlapping between the fluorescence emission spectrum of HSA (a) (λ_{ex} = 285 nm) and UV absorption spectrum of Ap (b), [HSA] = 1.0 μmol L^{-1}, [Ap] = 1.0 μmol L^{-1}, pH = 7.4, T = 298 K.

We observed that the UV absorption peak of Ap is in the range of fluorescence emission wavelength of HSA, so the fluorescence energy of HSA can be transferred to the molecule of Ap to exit the π–π transition of electron in the molecule of Ap on condition that the distance between Ap and HSA is enough close. E equal to 23.32% by the Eq. (7), and when K^2, N and $\emptyset$ is 2/3, 1.336 and 0.118 [26], J is 1.53×10^{-14} cm^3 L mol^{-1} from Eq. (9), R_0 is 2.63 nm, r_0 equal to 3.21 nm. According to Refs. [26,34], a non-radiation energy transfer between donor and acceptor can occur none but the maximal academic critical distance for R_0 is from 5 to 10 nm and the maximum academic distance for r_0 is in the range of 7 and 10 nm. In the study, R_0 and r_0 both are far lower than the corresponding maximum value, so the conclusion could be drawn that a non-radiation energy transfer occur between Ap and HSA.

3.7. Analysis of HSA conformation after Ap binding

We had ascertained that it is the binding of Ap to HSA to cause the fluorescence quenching of HSA, but it is still a puzzle about whether the binding affects the conformation and/or microenvironment of HSA. To further verify the binding of Ap to HSA and investigate HSA structure after Ap binding, the methods of synchronous fluorescence, UV and CD were utilized.

The methods of synchronous fluorescence is a kind of simple and effective means to measure the fluorescence quenching and the possible shift of the maximum emission wavelength λ_{max}, relative to the alteration of the polarity around the chromophore microenvironment. Δλ, representing the value of difference between excitation and emission wavelengths, is an important operating parameter, the synchronous fluorescence of HSA at Δλ = 15 and 60 nm is characteristic of Tyr and Trp residue, respectively[27,35]. When Δλ is set at 15 or 60 nm the shift of the λ_{max} and the fluorescence quenching of HSA imply the alteration of polarity microenvironment around Tyr or Trp residues and the state of Ap binding to HAS [27,36]. The synchronous fluorescence spectra of interaction between Ap and HSA were presented in the Fig. 9. A faint blueshift (∼1 nm) can be observed from Fig. 8A, and at the same time, the fluorescence intensity of HSA weakened regularly along with the adding of Ap, implying that Ap bonded to HSA and located in close proximity to the Tyr residues, the polarity near the tyrosine residues was decreased and so the hydrophobicity was increased faintly. When the hydrophobic part of Ap molecular is close enough to the phenyl moiety of Tyr, hydrophobicity near the tyrosine residues increases involuntarily. No any shift of the λ_{max} was shown in Fig. 9B but only a gradual quenching, indicating that Ap was closed to Trp residue but had no effect on the microenvironment around Trp residue, the alternative information is that during dynamic equilibrium the scatter of Ap molecular induced the quenching although Ap is not enough close to Trp.

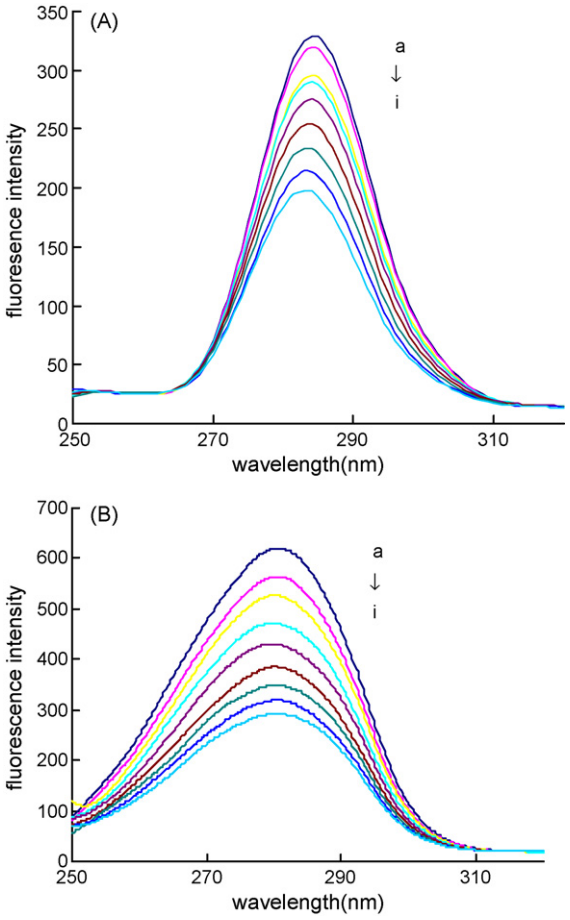

Fig. 9. Synchronous fluorescence spectra of interaction between HSA and Ap (A) at $\Delta\lambda$=15 nm. (B) at $\Delta\lambda$ = 60 nm. Concentrations of HSA was 1.0 μmol L^{-1} while concentrations of Ap were 0, 0.5, 1.0, 2.0, 4.0, 6.0, 8.0, 10.0, 12.0 μmol L^{-1} from the (a)–(i), pH 7.4, T = 293 K.

CD spectra of HSA exhibit two negative bands at 207 and 217 nm that is the characteristic of α-helix in the advanced structure of protein [37], if the α-helixes change the spectra will change accordingly. CD spectra of HSA without and with Ap were displayed in Fig. 10. No obvious change in band intensity and positions of the peaks could be observed even though the ratio of Ap to HSA is up to 20:1, giving the hint that addition of Ap had not altered secondary structure of HSA. From references some flavonoid altered secondary conformation of HSA after binding to the protein. The binding of alpinetin to HSA caused a dramatically decreasing in band intensity of CD spectrum of HSA [31], which is an indication of alteration of protein conformation. Although Ap and alpinetin are flavonoids, they have different characters. Firstly, their polarity is different. Ap is a flavonoid with 4′, 5, 7–OH but alpinetin has 7–OH and 5–OCH_3 on its main body, so Ap has stronger polarity than alpinetin. Secondly, their pKa is different. Ka of Alpinetin is 8.40 and so it is unionized at pH 7.4 but Ka of apigenin should be below that of alpinetin according to our experiments and so it is ionized partly. The characters may be very important factors on their binding to HSA and alteration of HSA after binding. The particular binding sites of Ap and alpinetin in HSA are different according to the results of modelling. Ap located to the entrance of site I with more positive charges but alpinetin binds to the hydrophobic cavity of site I formed by hydrophobic side chains, where alpinetin is faced to α-helix, So alpinetin is more possible to cause the alteration of HSA conformation than Ap. The main forces after Ap and alpinetin binding to HSA were different. The dominating forces of HAS–Ap are hydrophobic and electrostatic forces but the predominant force for alpinetin is only hydrophobic force, which are consistent with their characters. Differences of binding force may be one of reasons for alteration of HSA conformation.

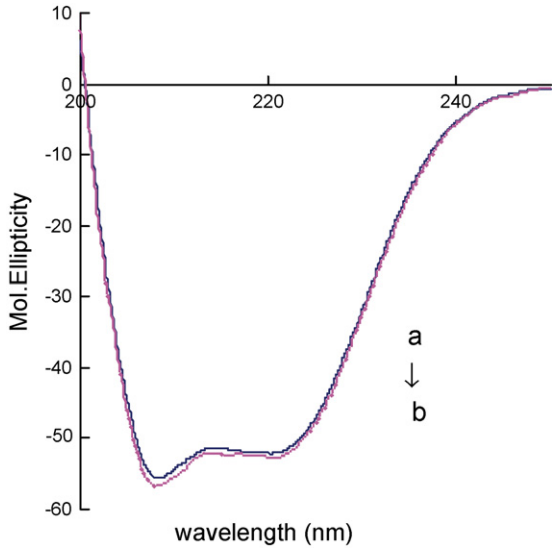

Fig. 10. CD spectra of HSA. (a) 5 μmol L^{-1} HSA; (b) 5 μmol L^{-1} HSA + 100 μmol L^{-1} Ap, pH 7.4, T = 293 K.

UV absorption spectra of HSA without and with binding of Ap (Fig. 11) were obtained by subtracting corresponding the spectrum of Ap-free form in the buffer from that of Ap–HSA complex, so only the spectra of HSA before and after binding Ap were showed in the Fig. 11. The absorption of HSA (∼210 nm)

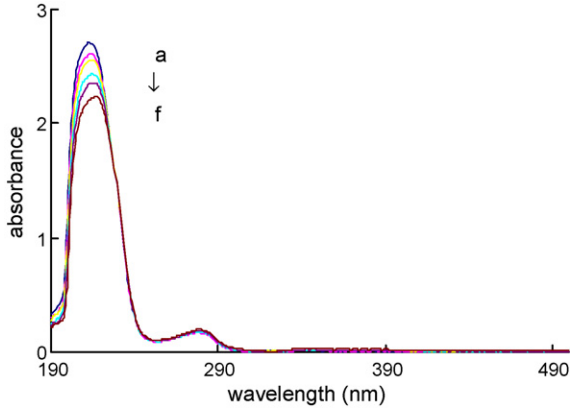

Fig. 11. UV absorption spectra of HSA in the absence and presence of Ap. Concentration of HSA was 5 μmol L^{-1} while concentration of Ap is 0, 5, 10, 15, 20, 25 μmol L^{-1} from the (a)–(f). The corresponding spectra of Ap in the buffer had been subtracted, respectively. pH 7.4, T = 288 K.

represents microenvironment or the content of α-helix structure of HSA [31,33]. The decrease of the absorption intensity of HSA at 213 nm and the shift from 213 to 217 nm with the increase of Ap concentration could be seen obviously, which suggested that the binding of Ap to HSA changed the microenvironment around HSA [33] but not secondary structure.

3.8. Molecular modeling of Ap binding to HAS

To further realize the information of the right site and interaction forces of Ap binding to HSA, Autodock 3.05 was applied to deduce the binding mode of Ap in HSA. Crystal structure of HSA shows that HSA is a heart-shaped helical monomer of 66 kD composed of three similar homologous domains named I (residues 1–195), II (196–383)and III (384–585) and each domain include two subdomains called A and B to form a cylinder and each subdomain involves 6 and 4 α-helixes, respectively, the only Trp residue (Trp^{214}) located in subdomain IIA [38]. Almost all hydrophobic amide acids are embedded in the cylinders and forming hydrophobic cavities, which play an important role on absorption, metabolism, and transportation of biomolecule. The three domains have similar 3D structure, and their assembly is highly asymmetric. Domain I and II are perpendicular to each other, forming a T-shaped assembly in which the tail of subdomain IIA is attached to the interface region between subdomain IA and IB by hydrophobic and hydrogen bonds [39]. Despite the internal structural symmetry of the three domains, they have different capacities for binding drugs. In the structure of HSA, there are two primary sites called site II (classical example is Warfarin) and site II (classical example is diazepam)for binding a wide variety of drug. The inside wall of the pocket of subdomain IIA corresponding to the so-called site I is formed by hydrophobic side chains, whereas the entrance of the pocket is surrounded by positively charged residues such as Arg^{257}, Arg^{222}, Lys^{199}, His^{242}, Arg^{218}, and Lys^{195}. Site II corresponds to the pocket with hydrophobic side chains in subdomain IIIA, which is almost the same size as site I. The third site in D-shaped cavity of subdomain IB named site III is typical for binding hemin [40]. Unlike subdomain IIA and IIIA, subdomain IA has no pocket near its hydrophobic core. In the subdomain IA, the fourth helix is flabby, so it is not able to keep parallel to the third helix and bury the putative pocket, but thanks to the interaction of subdomain IIIA with them, the region is sealed to form the site III. Although examples of drugs binding elsewhere on the protein have been reported, most investigations have focused on the three primary binding sites. HSA is a flexible protein that easily changes its molecular shape resulted from the relative motions of domain structures.

Through molecular modeling by Autodock 3.05, the optimum binding mode and site was displayed in the Fig. 12. It can be seen that the entrance of site I, a small cavity with positive-charged residues formed by interaction between subdomain IIA and IB, is the most possible binding site. Within 4 Å around Ap (Fig. 13), there are 16 amino acids residues and among them only two hydrophobic residues (Pro^{147}, Phe^{149}), five residues with positive charge (Lys^{106}, Arg^{197}, Lys^{199}, His^{242}, Arg^{257}) and the rest are polar residues (Gln^{29}, Tyr^{148}, Tyr^{150}, Gln^{196}, Cys^{200}, Cys^{245}, Cys^{246}, Gly^{248}, Cys^{253}). On account of the charge property of Ap under the physiological condition, it can be concluded that electrostatic force is one of the major forces of interaction between Ap and HSA. Furthermore, owing to the phenyl moiety of Phe^{149} exposed close to the A and C ring in Ap with additional aliphatic contact from Arg^{197}, His^{242} and Arg^{257}, in addition, phenyl of Tyr^{148} approach the ring B of Ap at nearly vertical orientation and Tyr^{150} is close tightly to the ring B of Ap at angle of about 60° from another side of Ap, it is concluded that hydrophobic force is another major force on the binding between Ap and HSA. Attributed to Ap binding to nearby (within 4 Å) Tyr^{148} and Tyr^{150}, the phenyl of Trp^{214} faced slantingly to the hydrophobic part in the side of A-ring in Ap, which suggested that when Ap

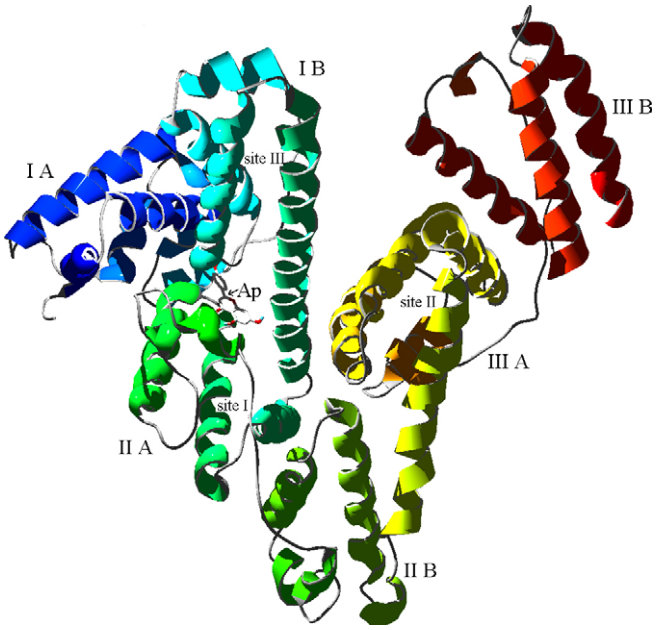

Fig. 12. Modeling of X-ray crystallographic structure of HSA complexed with Ap. The Ap was shown in the entrance of the site I. The domains and subdomains were displayed with different color, the every subdomain and classical binding site were marked in the corresponding location.

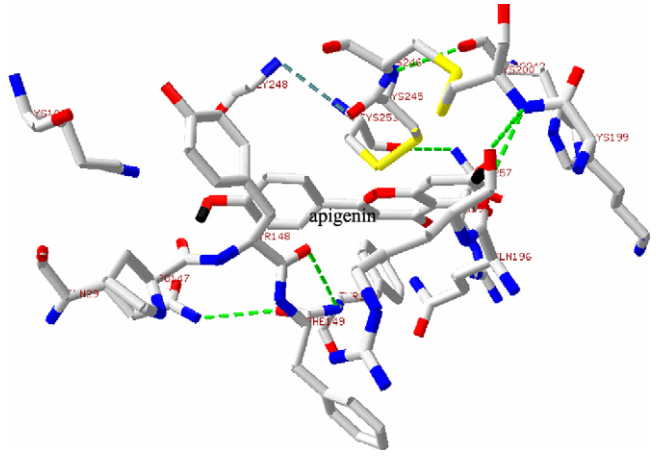

Fig. 13. The binding mode of Ap to HSA in the entrance of the site I. The displayed residues are within 4Å around Ap. The hydrogen bonds are shown by broken line.

move close enough to the Trp^{214} during the dynamic equilibrium the fluorescence energy of Trp can transfer to Ap to bring the quenching, so the fluorescence quenching of HSA induced by binding of Ap resulted from not only Tyr^{148} and Tyr^{150} but also Trp^{214}, which was agreed with the result of the synchronous fluorescence. According to references a wide range of biomolecules can be accommodated in the site I, and the interaction between biomolecules and HSA appears to be dominated by hydrophobic contacts, but there are a number of specific electrostatic interactions [41]. Main body of Ap molecule is hydrophobic but its surface is hydrophilic partly especially under pH above p*K*a of Ap. The results suggest unanimously that hydrophobic and electrostatic force play important role in the interaction between Ap and HSA. Many flavonoids such as quercetin bind in site I, so Ap is. Ap located in the entrance of site I but quercetin in the cavity of site I, the differences in the particular binding location should be resulted from the differences of characters of these ligands. Zsila et al. [24] reported that quercetin binds in the hydrophobic cavity of subdomain IIA in HSA and in the same site in BSA but caused the more efficient quenching of BSA owing to its second Trp. Dufour and Dangles proposed that flavonols binds mainly in the of subdomain IIA in serum albumin [42]. It is deserved to mention that there are more than one kind of binding mode between Ap and HSA but most of them are so instable that they disappear very soon and the phenomenon as factor of arising the fluorescence quenching of HSA carry through the dynamic equilibrium.

4. Conclusion

By spectroscopic and modeling methods, the interaction between Ap and HSA had been detected. The evident binding of Ap–HSA was resulted mainly from static mechanism by hydrophobic and electrostatic force in the entrance of site I in HSA but no hydrogen bond was found there, and the results of UV, fluorescence spectroscopy, synchronous fluorescence and molecular modeling gave the same information. The distance between Ap and HSA is enough close ($r_0 = 3.21$ nm) to arose non-radiation energy transfer from HSA to Ap. Owing to Ap binding to Tyr^{148} and Tyr^{150} of HSA within 4 Å and the close distance between Ap and Trp^{214}, the fluorescence quenching induced by binding of Ap to HSA was mainly brought by Tyr^{148}, Tyr^{150} and Trp^{214}, and the binding brought the alteration of microenvironment around Tyr in the region. The binding of Ap to HSA had not changed the secondary structure of HSA, as shown in the spectra of CD. The work provides some valuable information for the transportation and distribution of Ap in vivo, and is helpful for clarifying toxicity and dynamics of Ap.

Acknowledgements

The authors gratefully acknowledge the help from Dr. Zhong-Liang Zheng in the molecular modeling and analysis. The research was supported by grants from National Fund of Nature Science of China (NO.30670464) and The Research Fund for the Doctoral program of Higher Education of China (No.30370366).

References

[1] G. Galati, M.Y. Moridani, T.S. Chan, P.J. O'Brien, Free Radic. Biol. Med. 30 (2001) 370–382.
[2] B.H. Havsteen, Pharmacol. Ther. 96 (2002) 67–202.
[3] M.E. Gerritsen, W.W. Carley, G.E. Ranges, C.P. Shen, S.A. Phan, G.F. Ligon, C.A. Perry, Am. J. Pathol. 147 (1995) 278–292.
[4] Y.B. Ji, Publishing House of Sci. Tech., Heilongjiang, China, 1999.
[5] M. Ca'rdenas, M. Marder, V.C. Blank, L.P. Roguin, Bioorg. Med. Chem. 14 (2006) 2966–2971.
[6] A. Capasso, A. Pinto, R. Sorrentino, F. Capasso, J. Ethnopharmacol. 34 (1991) 279–281.
[7] G. Di Carlo, G. Autore, A.A. Izzo, P. Maiolino, N. Mascolo, P. Viola, M.V. Diurno, F. Capasso, J. Pharm. Pharmacol. 45 (1993) 1054–1059.
[8] Y.H. Zhang, et al., Gen. Pharmacol. 35 (2002) 341–347.
[9] J. Bektic, R. Guggenberger, B. Spengler, V. Christoffel, A. Pelzer, A.P. Berger, R. Ramonera, G. Bartsch, H. Klocker, Maturitas 55 (2006) S37–S46.
[10] L.C. Chiang, L.T. Ng, I-Ch. Lin, P.L. Kuo, Ch.Ch. Lin, Cancer Lett. 237 (2006) 207–214.
[11] T.D. Way, M.C. Kao, J.K. Lin, J. Biol. Chem. 279 (2004) 4479–4489.
[12] W. Wang, L. Heideman, C.S. Chung, J.C. Pelling, K.J. Koehler, D.F. Birt, Mol. Carcinog. 28 (2000) 102–110.
[13] I.K. Wang, S.Y. Lin-Shiau, J.K. Lin, Eur. J. Cancer 35 (1999) 1517–1525.
[14] M.A. Vargo, O.H. Voss, F. Poustka, A.J. Cardounel, E. Grotewold, A.I. Doseff, Biochem. pharmacol. 72 (2006) 681–692.
[15] H. Wei, L. Tye, E. Bresnick, D.F. Birt, Cancer Res. 50 (1990) 499–502.
[16] S. Caltagirone, C. Rossi, A. Poggi, F.O. Ranelletti, P.G. Natali, M. Brunetti, et al., Int. J. Cancer 87 (2000) 595–600.
[17] J. Psotova, S. Chlopcikova, P. Miketova, J. Hrbac, V. Simanek, Phytother. Res. 18 (2004) 516–521.
[18] Y. Li, W.Y. He, H.X. Liu, X.J. Yao, Zh.D. Hu, J. Mol. Struct. 831 (2007) 144–150.
[19] J.R. Lakowicz, G. Weber, Biochemistry 12 (1973) 4161–4170.
[20] K. Tang, Y.M. Qin, Ai-H. Lin, X. Hu, G.L. Zou, J. Pharm. Biomed. Anal. 39 (2005) 404–410.
[21] A.H. Lin. Thesis for Doctor degree, WuHan University, 2005.
[22] Zh.l. Zheng, Zh.Y. Zuo, Zh.G. Liu, K.Ch. Tsai, A.F. Liu, Zou.F G.L., J. Mol. Graph. Model. 23 (2005) 373–380.
[23] C.D. Kanakis, P.A. Tarantilis, M.G. Polissiou, S. Diamantoglou, H.A. Tajmir-Riahi, J. Mol. Struct. 798 (2006) 69–74.
[24] F. Zsila, Z. Bikádi, M. Simonyi, Biochem. Pharmacol. 65 (2003) 447–456.
[25] J.R. Lakowicz, Plenum Press, New York. 1983. pp. 257–265.
[26] Sh.Y. Bi, L. Ding, Y. Tian, D.Q. Song, X. Zhou, X. Liu, H.Q. Zhang, J. Mol. Struct. 703 (2004) 37–45.
[27] Y.Q. Wang, H.M. Zhang, G.Ch. Zhang, W.H. Tao, Sh.H. Tang, J. Mol. Struct. 830 (2007) 40–45.
[28] A. Sharma, S.G. Schulman, Wiley, New York, 1999.
[29] P.B. Kandagal, J. Seetharamappa, S.M.T. Shaikh, D.H. Manjunatha, J. Photochem. photobiol. A: Chem. 185 (2007) 239–244.
[30] G.Z. Chen, X.Z. Huang, J.G. Xu, Z.B. Wang, Z.X. Zheng, Method of Fluorescent Analysis, second ed., Science Press, Beijing, 1990.
[31] W.Y. He, Y. Li, Ch. X. Xue, Zh.D. Hu, X.G. Chen, F.L. Sheng, Bioorg. Med. Chem. 13 (2005) 1837–1845.
[32] D.P. Ross, S. Sabramanian, Biochemistry 20 (1981) 3096.
[33] W.Y. He, Y. Li, H.Z. Si, Y.M. Dong, F.L. Sheng, X.J. Yao, Zh.D. Hu, J. Photochem. Photobiol. A: Chem. 182 (2006) 158–167.
[34] G.Z. Chen, X.Z. Huang, J.G. Xu, Z.B. Wang, Z.Z. Zheng, Method of Fluorescent Analysis, second ed., Science Press, BeiJing, 1990.
[35] T. Yuan, A.M. Weljie, H.J. Vogel, Biochemistry 37 (1998) 3187.
[36] W.C. Abert, W.M. Gregory, G.S. Allan, Anal. Biochem. 213 (1993) 407–413.
[37] Q.Q. Bian, J.Q. Liu, J.N. Tian, Zh.D. Hu, Int. J. Biol. Macromol. 34 (2004) 275–279.

[38] J.H. Tang, F. Luan, X.G. Chen, Bioorg. Med. Chem. 14 (2006) 3210–3217.
[39] S. Sugio, A. Kashima, S. Mochizuki, M. Noda, K. Kobayashi, Protein Eng. 12 (1999) 439–446.
[40] P.A. Zunszain, J. Ghuman, T. Kornatsu, E. Tsuchida, S. Curry, BMC Struct. Biol. (2003) 7.
[41] I. Petitpas, A.A. Bhattacharya, S. Twine, M. East, S. Curry, J. Boil. Chem. 276 (2001) 22804–22809.
[42] C. Dufour, O. Dangles, Biochim. Biophys. Acta 1721 (2005) 164–173.